International Journal of Chemical and Biochemical Sciences
(ISSN 2226-9614)

Journal Home page: www.iscientific.org/Journal.html

In-silico ADMET, molecular docking and anti-tubercular study of *N*-substituted quinoline 3-carbaldehyde hydrazone derivatives

Nilesh M. Jangade[1*], Manoj S. Charde[2]

[1]Assistant Professor, Department of Pharmaceutical Chemistry, Bharati Vidyapeeth College of Pharmacy, Palus, Maharashtra, India*

[2]Assistant Professor, Department of Pharmaceutical Chemistry, Government College of Pharmacy, Karad, Maharashtra, India

Abstract

A computational modeling method called molecular docking is used to build complexes between interacting molecules. Its fundamental objective is to forecast a molecule's three-dimensional structure in order to comprehend its interactions and prospective therapeutic uses. In silico investigations were carried out on ADMET using the web tools SWISS ADME, Molinspiration, and AdmetSAR. This study focuses on investigating the binding mode, interactions against mycobacterial ATP synthaze using virtual screening conducted with AutoDock 4.2 and potential anti-tubercular activity of new *N*-substituted Quinoline 3-carbaldehyde hydrazone derivatives. Derivatives 4d, 5a, 5b, 7b and 7d exhibited strong binding interaction with target ATP synthaze. Compound 5b and 7b shown excellent antitubercular activity with MIC value of 0.8 µg/ml comparing with standard drug Isoniazid MIC value of 1.6 µg/ml.

Keywords: Quinoline 3-carbaldehyde hydrazone, ATP synthaze, Molecular docking, Anti-tubercular activity.

Full length article **Corresponding Author*, e-mail: nilesh.jangade01@gmail.com

1. Introduction

An in-silico technique called molecular docking detects the proper binding pose of a protein-ligand combination. It assesses its effectiveness using a variety of scoring methods to determine the optimal pose produced by each molecule [1]. Optimizing variables including hydrophobic, steric and electrostatic as well as calculating their binding free energies, docking approaches try to fit a ligand into the binding site of the target protein [2]. Protein data bank (PDB) was used to derive 3D protein structures [3]. In order to build complexes between molecules that interact, computational modeling is used in molecular docking. The basic objective is to predict the three-dimensional structure of an interest. The application of molecular docking software is mainly focused on enhancing drugs, enabling the efficient design and analysis of pharmaceuticals. Through molecular docking, virtual screening of extensive compound libraries is made possible, allowing for result ranking and proposing structural hypotheses for lead optimization in drug development. Tuberculosis, caused by the Mycobacterium Tuberculosis (MTB), is a chronic lung disease. It is considered one of the deadliest diseases, particularly when occurring alongside HIV infection, posing a massive threat to mankind. The global occurrence of TB is primarily driven by two factors: Multidrug-resistant tuberculosis (MDR-TB) and the Acquired Immuno deficiency Syndrome [4]. The majority of TB cases are reported from developing nations, and the number of HIV-positive people who also have TB is increasing. 10.6 million Persons were reportedly infected with TB in 2021, up from 10.1 million cases (or 4.5%) in 2020. During the same period, the incident rate of TB rose by 3.6%, resulting in approximately 187 thousand deaths among HIV-positive individuals [5]. Quinoline is commonly found in natural compounds and serves as a precursor for numerous synthetic derivatives with diverse pharmacological activities, including antimalarial, antihypertensive, anticancer and antifungal properties [6-10]. The presence of both non-polar and polar moieties in new *N*-substituted quinoline 3-carbaldehyde hydrazone derivatives makes it suitable for permeation into bacterial cells [11]. Molecular docking focuses on computational procedure of finding and appropriate binding of ligand and receptor. In this study, virtual screening with AutoDock 4.2 was used to examine the binding mechanism and interaction of new *N*-substituted quinoline 3-carbaldehyde hydrazone derivatives Table 1 with the mycobacterial ATP synthaze.

The ATP synthaze is a key metabolic enzyme required for ATP generation. Therefore, ATP synthaze is considered a viable target in the current study to find anti-tubercular drugs.

2. Materials and Methods

2.1. Preparation of ligands

Chemdraw software was used to design the derivatives' 2D and 3D possible structures. These sketched structures were subsequently converted using pymol software into the PDB format, which was used for ADMET screening and docking studies.

2.2. Selection and preparation of protein

Using the Swiss Target Prediction Report as a guide, the ATP synthaze was selected for the docking investigation. The PDB was used to retrieve the three-dimensional crystallographic structure of ATP synthaze.

2.3. Predictions of pharmacokinetics (ADME) and toxicology

The ADME and toxicological characteristics of bioactive molecules were predicted using Molsoft, Molinspiration and Swiss ADME tools. Based on the compound's structure, these tools compute pharmacokinetic and toxicological characteristics.

2.4. Bioactive molecule's drug likeness score

The drug similarity of each compound was assessed using Molsoft, Molinspiration, and Swiss ADME online servers, which consider factors such as atomic weight, the total number of H-donors and H-acceptors, and log P.

2.5. Protein-ligand docking

Molecular docking was carried out using AutoDock 4.2. The protein structure included water molecules, hydrogen atoms, and Kollman charges. The docking process was then completed after defining a grid box. The dlg file was used to determine the ideal ligand pose based on the binding energy after docking. In order to depict the interaction between the ligand and the protein, Biovia ultimately chose the position with the lowest binding energy.

2.6. ADME prediction and drug likeliness study

Computational research of titled substances was performed to estimate their ADME properties. Researchers utilized the online web tools SWISS ADME and Molinspiration for property calculations, including Log P, total polar surface area (TPSA), molecular volume, number of rotatable bonds, and the number of hydrogen donor and acceptor atoms. For drug design, the concept of drug-likeness is employed. To assess drug-likeness, the Lipinski rule of five is considered taking into account molecular weight, hydrophobicity and the number of hydrophilic groups. The tool used is SWISS ADME Web to evaluate synthetic compounds for its drug-likeness features.

2.7. In-silico pharmacokinetics and toxicity prediction

AdmetSAR software was employed to estimate the various ADMET characteristics of the most well-known compound. The AMES toxicity test was utilized to assess the mutagenicity of the compound. The processed ligand showed a negative AMES toxicity test result for the compound, indicating that it is non-mutagenic. Furthermore, the virtual screening chemical exhibited a lower value and was found to be non-carcinogenic. For in silico pharmacokinetic prediction, the SWISS ADME online web tool was utilized. The tool predicted the gastrointestinal absorption and oral bioavailability of the compounds.

2.8. Computational Methodology

Using virtual screening with AutoDock4.2, the binding mechanism and interaction of new *N*-Substituted Quinoline 3-Carbaldehyde hydrazone derivatives with the mycobacterial ATP synthaze were investigated [12]. Using the source code 4V1F.pdb, the crystal structure of ATP synthaze was obtained from the RCSB database. An innovative, Mycobacterium-specific adenosine triphosphate (ATP) synthaze inhibitor is called Bedaquiline (BDQ). The mycobacterial ATP synthaze's membrane-embedded rotor (c-ring) is the target of the BDQ substance. A vital metabolic enzyme needed for the production of ATP is the ATP synthaze. Therefore, ATP synthaze is considered a viable target in the current study to find anti-tuberculosis medications. new *N*-Substituted Quinoline 3-Carbaldehyde hydrazone derivatives compounds' atomic coordinates were created using the Discovery studio visualizer. In this case, AutoDock4.2 software treats the BDQ binding site as the active site of ATP synthaze for virtual screening. For molecular docking for new *N*-Substituted Quinoline 3-Carbaldehyde hydrazone derivatives, the grid box of 40 x 40 x40 and a grid spacing of 0.375 were taken into consideration. The 4VIF receptor protein was kept rigid for docking while the pharmacological component was made of a flexible molecule. The default settings for the Lamarckian genetic algorithm were employed [13]. A further classification of drug output conformations was made using an all-atom RMSD with a cut-off of 4. Following earlier research, the binding energy, cluster size, intermolecular energy, and van der Waals energy of these output conformations were then compared [14-17]. In the least energy binding conformation of new *N*-Substituted Quinoline 3-Carbaldehyde hydrazone derivatives with ATP synthaze, more study was conducted on bonding interactions, van der Waals contacts, and electrostatic interactions.

2.9. Anti-tubercular activity

All the synthesized compounds were passed for anti-tubercular activity using the microplatealamar blue assay against M. tuberculosis H37Rv.

3. Results and Discussion

3.1. In-silico approach for ADME study and drug likeness prediction

A compound's physicochemical properties are carefully studied when determining how drug-like it is to see if they meet standards like the Lipinski rule of five. Various factors are considered, encompassing features like topological polar surface area (TPSA), logP, hydrogen bond donors (HBD), count of rotatable bonds, molecular mass, molar refractivity, quantity of rotatable bonds, and hydrogen bond acceptors (HBA).

The results, presented in Table 2, provide a summary indicating that all derivatives strictly adhere to the Lipinski

Rule of Five without any breaches. Molecular modeling software was employed to forecast the bioactivity of synthesized compounds. By evaluating bioactivity scores, a comparison was made between the isolated compounds and established drugs across protease inhibitors (PI), kinase inhibitors (KI), ion channel modulators (ICM), GPCR ligands (GPCRL), nuclear receptor ligands (NRL) and enzyme inhibitors (EI). Table 3 presents the findings of the bioactivity assessment.

3.2. In silico pharmacokinetic and toxicity prediction

Pharmacokinetics prediction study like GI absorption, Caco absorption, p-gp, CYP2C19 Inhibitor, CYP2D6 Inhibitor mentioned in Table 4 was done on SwissADME. Toxicity prediction study like ames mutagenesis, carcinogenicity, acute oral toxicity and acute toxicity LD 50 mentioned in Table 5 was done on Admet SAR software.

3.3. Molecular docking results

The investigation of ATP-synthaze and 5b revealed, as indicated in Table 6 and Figure 3, that the 5b is stabilized by its hydrogen bonding contact with Phe58 (2.52). Additionally, the 5b forms non-bonded interactions with Val61 and Leu63 of the stacked and -alkyl types (Figure 3). To investigate the binding affinity and interaction of potential new *N*-substituted quinoline 3-carbaldehyde hydrazone derivatives, virtual screening was performed using Auto Dock Vina software. The docking analysis showed that the compound 4d, 5a, 5b, 7b and 7d found to be higher affinity with the ATP synthaze as shown Table 6. These least binding energy five new *N*-substituted quinoline 3-carbaldehyde hydrazone derivatives were further analyzed for binding mode and 2D interaction analysis using PyMol and Discovery studio Visualizer, respectively [18-21].

3.4. In-vitro anti-tubercular screening

Microplate alamar blue assay was used to assesses anti-tubercular activity of new *N*-substituted quinoline 3-carbaldehyde hydrazone derivatives. The minimum inhibitory concentration (MIC) values of the new *N*-Substituted Quinoline 3-Carbaldehyde hydrazone derivatives and standard drug isoniazid mentioned in the Table 7.

Table 1: New *N*-substituted quinoline 3-carbaldehyde hydrazone derivatives.

Compound	Structure	Compound	Structure
4d	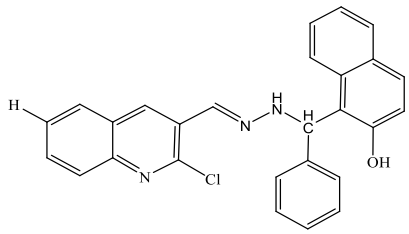	7b	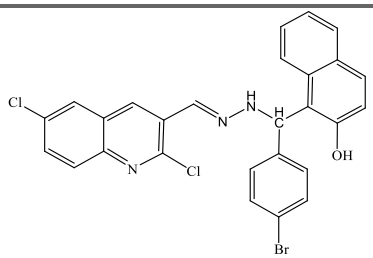
5a	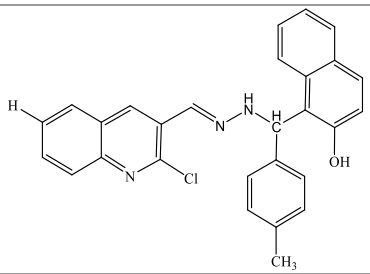	7d	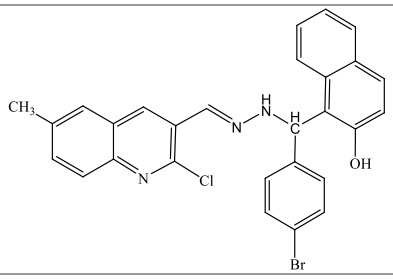
5b	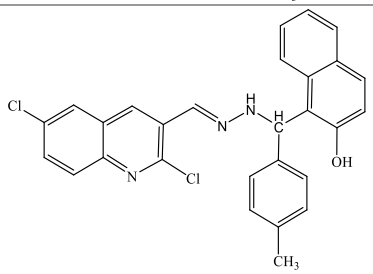		

Table 2: The synthesized compounds were evaluated for lipinski parameters.

Comp.	Physicochemical Properties						Drug Likeness		
	Mol. Wt.	H-accepter	H-donor	Rotatable bond	Log *p*	Total polar surface area (TPSA)	Lipinski violations	Bioavailability Score	Synthetic Accessibility
4d	437.92	3	2	5	3.85	57.51	01	0.55	3.61
5a	451.95	3	2	5	4.06	57.51	01	0.55	3.72
5b	486.39	3	2	5	4.42	57.51	01	0.55	3.74
7b	551.26	3	2	5	4.51	57.51	02	0.17	3.70
7d	530.84	3	2	5	4.64	57.51	02	0.17	3.80

Table 3: Molinspiration bioactivity score.

Comp.	GPCR ligand	Ion channel modulator	Kinase Inhibitor	Nuclear receptor ligand	Protease inhibitor	Enzyme inhibitor
4d	-0.15	-0.25	-0.23	-0.23	-0.34	-0.14
5a	-0.18	-0.30	-0.26	-0.24	-0.37	-0.18
5b	-0.18	-0.30	-0.26	-0.25	-0.37	-0.19
7b	-0.22	-0.30	-0.26	-0.31	-0.41	-0.20
7d	-0.25	-0.35	-0.29	-0.32	-0.45	-0.23

Table 4: Pharmacokinetic prediction using SWISS ADME.

Compound	GI Absorption	Caco absorption	p-gp	CYP2C19 Inhibitor	CYP2D6 Inhibitor
4d	High	Yes	No	No	No
5a	High	Yes	No	No	No
5b	Low	Yes	No	No	No
7b	Low	Yes	Yes	No	No
7d	Low	Yes	No	No	No

Table 5: Toxicity prediction using Admet SAR software.

Compound	Ames Mutagenesis	Carcinogenicity	Acute Oral Toxicity	Acute Toxicity LD50 mol/Kg
4d	+0.5400	-0.6957	III 0.5021	2.608
5a	+0.5700	-0.6857	III 0.5308	2.608
5b	+0.5700	-0.6857	III 0.5308	2.696
7b	+0.5500	-0.7057	III 0.5178	2.669
7d	+0.5600	-0.6957	III 0.5401	2.392

Table 6: Hydrogen bonding interaction of *N*-substituted quinoline 3-carbaldehyde hydrazone derivatives with ATP synthaze using molecular docking.

Comp.	Binding energy in Kcal. mol	Atoms involved in the bonding	Distance	Angle	Interactions Type
4d	-8.5	4d-H13 - B: PHE 58:O GLU65:OE1 – 4d GLU65:OE1 – 4d PHE58 – 4d PHE58 – 4d 4d -O - A: LEU 63 4d -O - B: VAL 61	2.4217 3.50486 3.39744 4.59046 3.68109 4.93357 4.92959	132.928	Hydrogen Bond Pi-Anion Pi-Anion Pi-Pi Stacked Pi-Pi Stacked Pi-Alkyl Pi-Alkyl
5a	-8.5	5a:H13 - B: PHE 58:O B: GLU65: OE1 – 5a B: GLU65: OE1 – 5a B: PHE58 –5a B: PHE58 – 5a 5a -C34 - A: ILE59 5a -C34 - A: LEU63 5a - A: LEU63 5a - B: VAL61	2.42168 3.41537 3.37866 4.6802 3.72858 4.34494 4.11531 5.04983 5.17793	145.765	Hydrogen Bond Pi-Anion Pi-Anion Pi-Pi Stacked Pi-Pi Stacked Alkyl Alkyl Pi-Alkyl Pi-Alkyl
5b	-8.6	5b:H12 - B: PHE58:O B: GLU65:OE1 – 5b B: GLU65: OE1 – 5b B: PHE58: HB2 – 5b B: PHE58 – 5b B: PHE58 – 5b B: PHE58 – 5b 5b -CL11 - B: LEU72 5b -C34 - A: ILE59 5b -C34 - A: LEU63 B: TYR68 - 5b -CL11 B: PHE69 - 5b -CL11 5b - A: LEU63 5b - B: VAL61	2.52619 3.46988 3.44174 2.60096 4.99613 3.82354 5.12144 4.34341 4.2936 4.25705 4.73895 4.67174 5.25466 5.01253	149.494	Hydrogen Bond Pi-Anion Pi-Anion Pi-Sigma Pi-Pi Stacked Pi-Pi Stacked Pi-Pi T-shaped Alkyl Alkyl Alkyl Pi-Alkyl Pi-Alkyl Pi-Alkyl Pi-Alkyl
7b	-8.5	B: PHE58 – 7b B: PHE58 - 7b B: PHE58 - 7b B: ALA66 - 7b -CL11 7b -CL11 - B: ILE70 7b -BR34 - A: LEU63 7b -BR34 - B: VAL61 B: PHE69 – 7b-CL11 7b - B: ALA66 7b - B: VAL61 7b - B: ILE59	4.76697 4.20889 5.97958 3.84855 5.39236 4.1959 4.57143 5.17765 4.26356 5.42876 5.37358		Pi-Pi Stacked Pi-Pi Stacked Pi-Pi Stacked Alkyl Alkyl Alkyl Alkyl Pi-Alkyl Pi-Alkyl Pi-Alkyl Pi-Alkyl
7d	-8.5	7b-H15 - B: PHE58:O B: PHE58 - 7d B: PHE58 - 7d B: PHE58 - 7d B: PHE69 - 7d 7d -BR34 - A: LEU63 7d BR34 - B: VAL61 B: PHE58 - 7d -BR34 B: PHE69 - 7d -C11 7d - B: VAL61	2.32632 5.30181 4.31784 4.52485 4.98718 4.44926 4.79666 5.32973 3.71762 5.2401	93.499	Hydrogen Bond Pi-Pi Stacked Pi-Pi Stacked Pi-Pi Stacked Pi-Pi T-shaped Alkyl Alkyl Pi-Alkyl Pi-Alkyl Pi-Alkyl

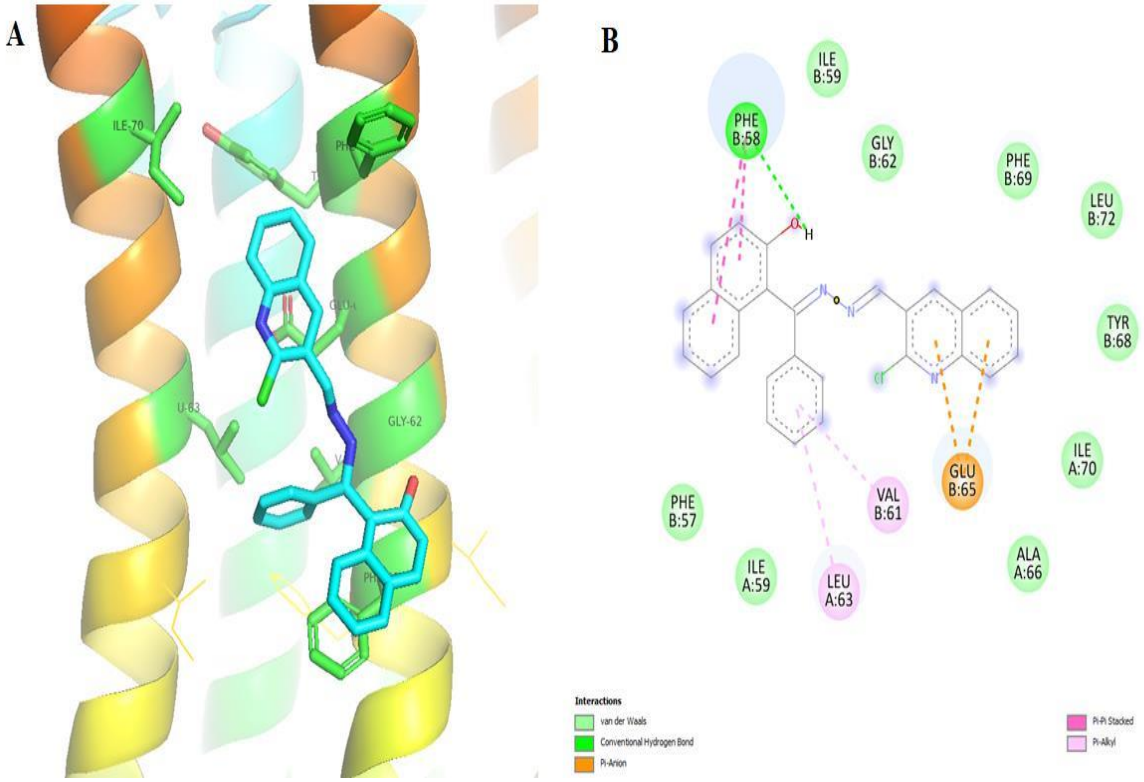

Figure 1: Binding mode of ATP synthaze with 4d. Here (A) shows the binding pocket of 4d and (B) shows the interaction network of 4d with ATP synthaze residues using Discovery studio Visualizer.

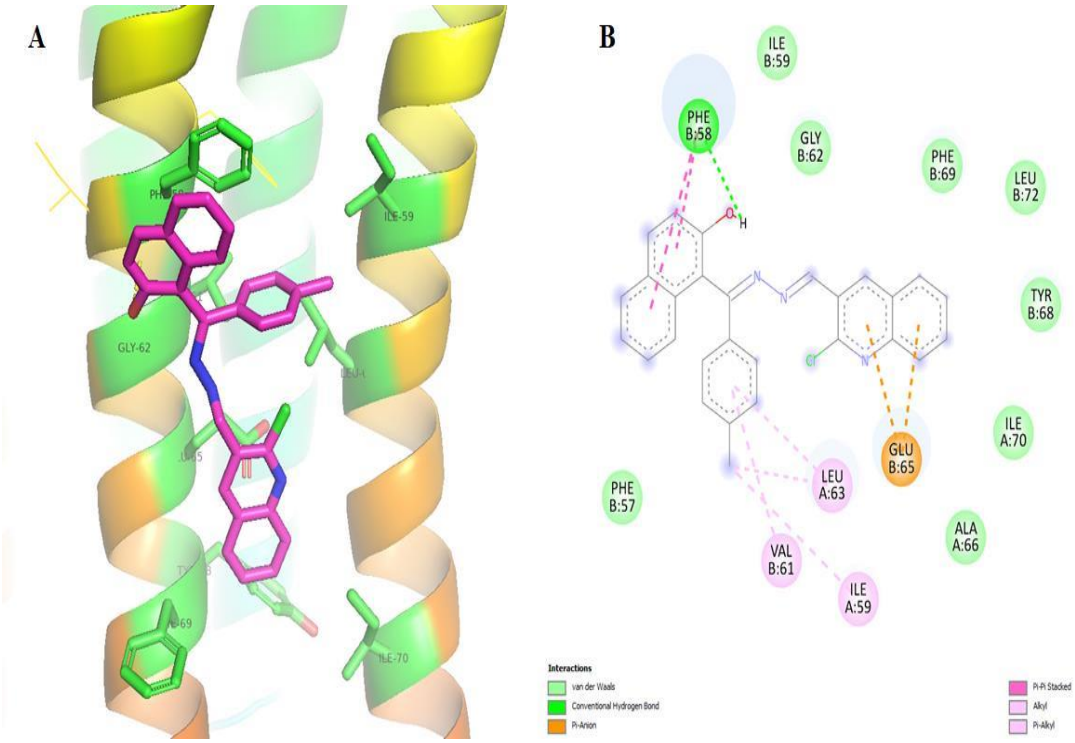

Figure 2: Binding mode of ATP synthaze with 5a. Here (A) shows the binding pocket of 5a and (B) shows the interaction network of 5a with ATP synthaze residues using Discovery studio Visualizer.

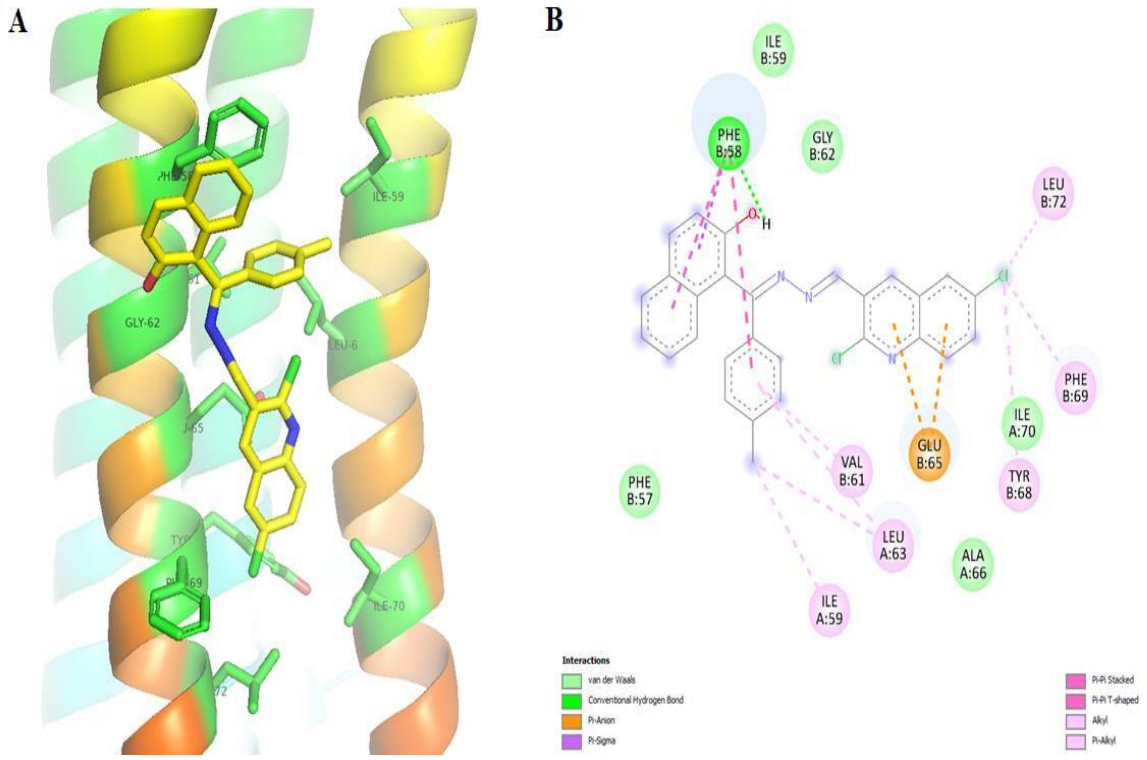

Figure 3: Binding mode of ATP synthaze with 5b. Here (A) shows the binding pocket of 5b and (B) shows the interaction network of 5b with ATP synthaze residues using Discovery studio Visualizer.

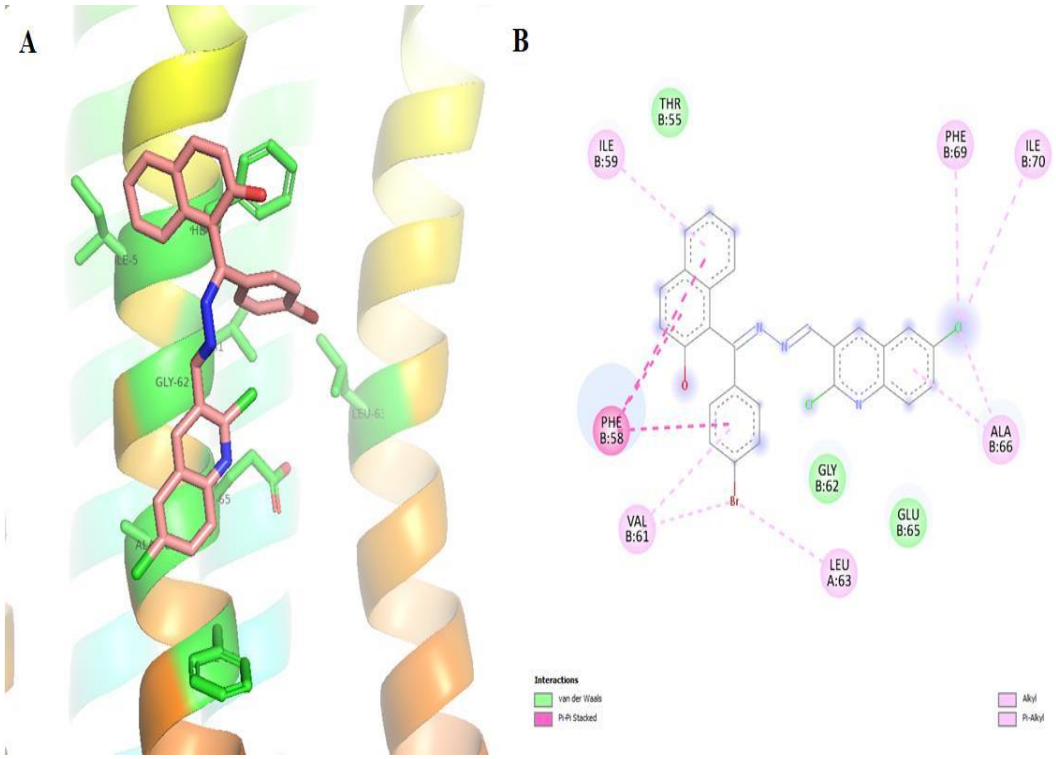

Figure 4: Binding mode of ATP synthaze with 7b. Here (A) shows the binding pocket of 7b and (B) shows the interaction network of 7b with ATP synthaze residues using Discovery studio Visualizer.

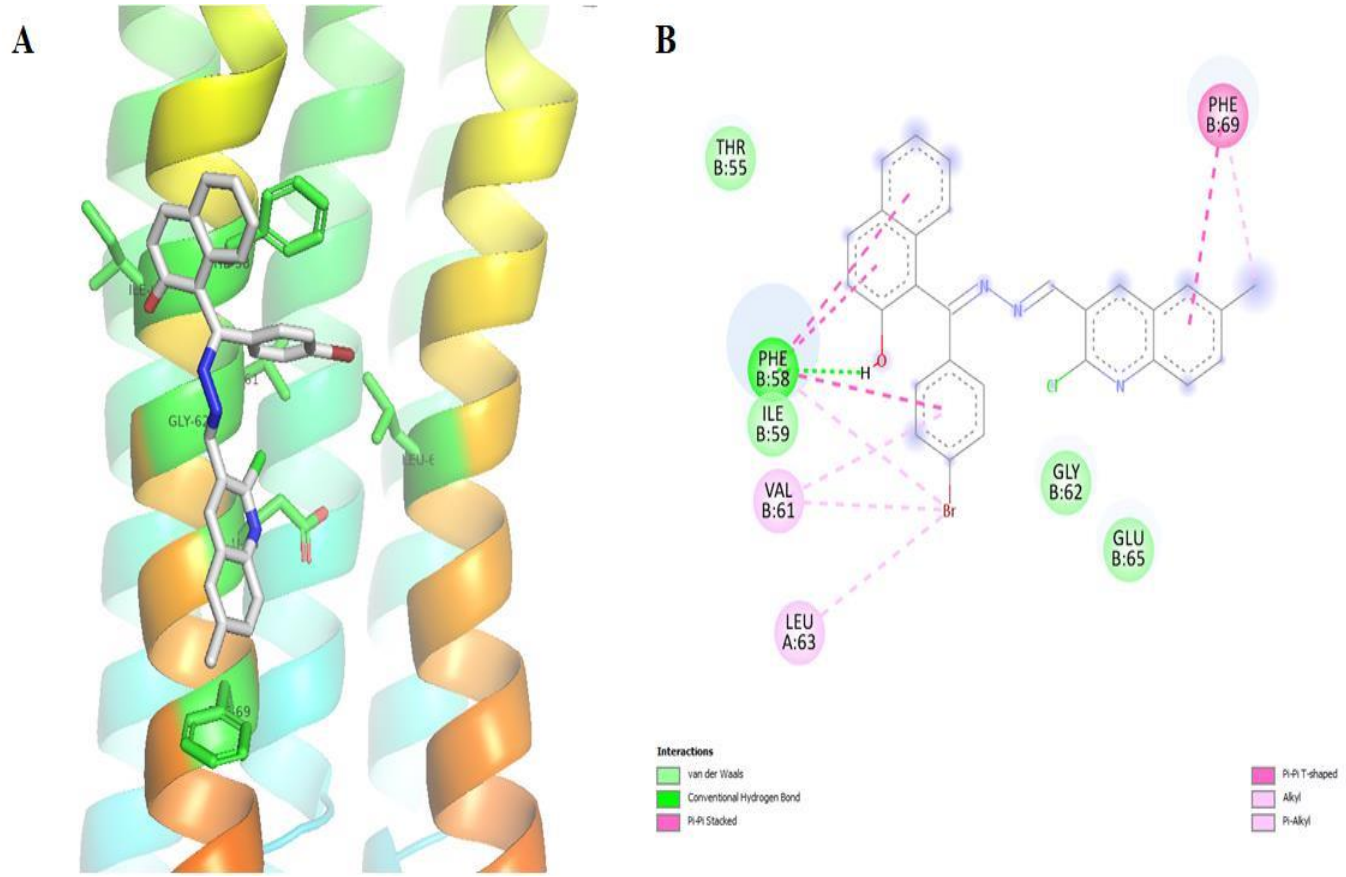

Figure 5: Binding mode of ATP synthaze with 7d. Here (A) shows the binding pocket of 7d and (B) shows the interaction network of 7d with ATP synthaze residues using discovery studio visualizer.

Table 7: Anti-tubercular screening of new *N*-substituted quinoline 3-carbaldehyde hydrazone derivatives.

Comp.	*M. tuberculosis* $H_{37}Rv$ MIC (µg/ml)	Comp.	*M. tuberculosis* $H_{37}Rv$ MIC (µg/ml)
4d	1.6	7b	0.8
5a	1.6	7d	1.6
5b	0.8	Isoniazid	1.6

4. Conclusions

Above ADME study suggest that all the drugs are safe and are not carcinogenic in nature. The utilization of molecular docking offers a cost-effective, safe, and user-friendly approach for exploring, interpreting, explaining, and uncovering molecular characteristics within three-dimensional structures. Docking is a method employed to predict the structural interactions between new *N*-Substituted Quinoline 3-Carbaldehyde hydrazone derivatives and ATP synthaze. Compounds 4d, 5a, 5b, 7b and 7d shown that they have good binding interaction with target ATP synthaze. These derivatives may turn out to be potential anti-tubercular drugs.

Acknowledgement

Authors immensely thankful to Bharati Vidyapeeth College of Pharmacy, Palus and Government College of Pharmacy, Karad Maharashtra, India for providing facilities for research work and their constant support.

Competing of Interest

The Authors have stated that they have no competing interests.

References

[1] I. D. Kuntz, J. M. Blaney, S. J. Oatley, R. Langridge, T. E. Ferrin. (1982). A geometric approach to macromolecule-ligand interactions. Journal of molecular biology. 161 (2): 269-288.

[2] D. J. Diller, K. M. Merz Jr. (2001). High throughput docking for library design and library prioritization. Proteins: Structure, Function, and Bioinformatics. 43 (2): 113-124.

[3] M. L. Teodoro, L. E. Kavraki. (2003). Conformational flexibility models for the receptor in structure-based drug design. Current pharmaceutical design. 9 (20): 1635-1648.

[4] S. D. Joshi, N. Tigadi, D. Kumar, S. R. Dixit, N. M. Jangade. (2016). Synthesıs of some novel pyrrolyl hydrazone derıvatıves as an antıtubercular agents. Indıan Journal of Heterocyclıc Chemıstry. 25 (3-4): 237-241.

[5] World Health Organization, Global Tuberculosis Report. (2022). 1-49. https://iris.who.int/bitstream/handle/10665/363752/9789240061729-eng.pdf?sequence=1.

[6] S. D. Joshi, N. M. Jangade, S. R. Dixit, A. S. Joshi, V. H. Kulkarni. (2016). Quinoline: a promising and versatile scaffold for future. American Journal of Pharmaceutical Research. 6 (04): 5033-5044.

[7] M. Foley, L. Tilley. (1998). Quinoline antimalarials: mechanisms of action and resistance and prospects for new agents. Pharmacology & therapeutics. 79 (1): 55-87.

[8] H. Kumar, V. Devaraji, R. Joshi, M. Jadhao, P. Ahirkar, R. Prasath, P. Bhavana, S. K. Ghosh. (2015). Antihypertensive activity of a quinoline appended chalcone derivative and its site-specific binding interaction with a relevant target carrier protein. RSC advances. 5 (80): 65496-65513.

[9] T. Nakamura, M. Oka, K. Aizawa, H. Soda, M. Fukuda, K. Terashi, K. Ikeda, Y. Mizuta, Y. Noguchi, Y. Kimura, T. Tsuruo. (1999). Direct interaction between a quinoline derivative, MS-209, and multidrug resistance protein (MRP) in human gastric cancer cells. Biochemical and biophysical research communications. 255 (3): 618-624.

[10] R. Musiol, J. Jampilek, V. Buchta, L. Silva, H. Niedbala, B. Podeszwa, A. Palka, K. Majerz-Maniecka, B. Oleksyn, J. Polanski. (2006). Antifungal properties of new series of quinoline derivatives. Bioorganic & Medicinal Chemistry. 14 (10): 3592-3598.

[11] M. C. Mandewale, U. C. Patil, S. V. Shedge, U. R. Dappadwad, R. S. Yamgar. (2017). A review on quinoline hydrazone derivatives as a new class of potent antitubercular and anticancer agents. Beni-Suef University journal of basic and applied sciences. 6 (4): 354-361.

[12] O. Trott, A. J. Olson. (2010). AutoDock Vina: improving the speed and accuracy of docking with a new scoring function, efficient optimization, and multithreading. Journal of computational chemistry. 31 (2): 455-461.

[13] B. V. Kumbhar, V. V. Bhandare. (2021). Exploring the interaction of Peloruside-A with drug resistant αβII and αβIII tubulin isotypes in human ovarian carcinoma using a molecular modeling approach. Journal of Biomolecular Structure and Dynamics. 39 (6): 1990-2002.

[14] B. V. Kumbhar, A. Borogaon, D. Panda, A. Kunwar. (2016). Exploring the origin of differential binding affinities of human tubulin isotypes αβII, αβIII and αβIV for DAMA-colchicine using homology modelling, molecular docking and molecular dynamics simulations. PLoS One. 11 (5): e0156048.

[15] B. M. Chougala, S. Samundeeswari, M. Holiyachi, L. A. Shastri, S. Dodamani, S. Jalalpure, S. R. Dixit, S. D. Joshi, V. A. Sunagar. (2017). Synthesis, characterization and molecular docking studies of substituted 4-coumarinylpyrano [2, 3-c] pyrazole derivatives as potent antibacterial and anti-inflammatory agents. European journal of medicinal chemistry. 125: 101-116.

[16] B. Sever, K. Kucukoglu, H. Nadaroglu, M. D. Altıntop. (2019). In silico Molecular Docking and ADME Studies of 1, 3, 4-Thiadiazole Derivatives in Relation to in vitro PON1 Activity. Current Computer-Aided Drug Design. 15 (2): 136-144.

[17] A. Daina, O. Michielin, V. Zoete. (2019). SwissTargetPrediction: updated data and new features for efficient prediction of protein targets of small molecules. Nucleic acids research. 47 (W1): W357-W364.

[18] W. L. DeLano. (2002). Unraveling hot spots in binding interfaces: progress and challenges. Current opinion in structural biology. 12 (1): 14-20.

[19] A. A. Shah, S. Ahmad, M. K. Yadav, K. Raza, M. A. Kamal, S. Akhtar. (2024). Structure-based virtual screening, molecular docking, molecular dynamics simulation, and metabolic reactivity studies of quinazoline derivatives for their anti-EGFR activity against tumor angiogenesis. Current Medicinal Chemistry. 31 (5): 595-619.

[20] M. Cheminformatics. (2014). Bratislava, Slovak Republic.

[21] C. A. Lipinski, F. Lombardo, B. W. Dominy, P. J. Feeney. (1997). Experimental and computational approaches to estimate solubility and permeability in drug discovery and development settings. Advanced drug delivery reviews. 23 (1-3): 3-25.